Full length article

New concentration-response functions for seven morbidity endpoints associated with short-term PM$_{2.5}$ exposure and their implications for health impact assessment

Muye Ru [a,b,*], Drew Shindell [a,c], Joseph V. Spadaro [d], Jean-François Lamarque [e], Ariyani Challapalli [a], Fabian Wagner [f], Gregor Kiesewetter [f]

[a] *Nicholas School of the Environment, Duke University, Durham, NC, USA*
[b] *Now at The Earth Institute, Columbia University, New York, NY, USA*
[c] *Porter School of the Environment and Earth Sciences, Tel Aviv University, Tel Aviv, Israel*
[d] *Spadaro Environmental Research Consultants, Philadelphia, PA, USA*
[e] *National Center for Atmospheric Research, Boulder, CO, USA*
[f] *International Institute for Applied Systems Analysis, Laxenburg, Austria*

ARTICLE INFO

ABSTRACT

Background: Morbidity burdens from ambient air pollution are associated with market and non-market costs and are therefore important for policymaking. The estimation of morbidity burdens is based on concentration–response functions (CRFs). Most existing CRFs for short-term exposures to PM$_{2.5}$ assume a fixed risk estimate as a log-linear function over an extrapolated exposure range, based on evidence primarily from Europe and North America.

Objectives: We revisit these CRFs by performing a systematic review for seven morbidity endpoints previously assessed by the World Health Organization, including data from all available regions. These endpoints include all cardiovascular hospital admission, all respiratory hospital admission, asthma hospital admission and emergency room visit, along with the outcomes that stem from morbidity, such as lost work days, respiratory restricted activity days, and child bronchitis symptom days.

Methods: We estimate CRFs for each endpoint, using both a log-linear model and a nonlinear model that includes additional parameters to better fit evidence from high-exposure regions. We quantify uncertainties associated with these CRFs through randomization and Monte Carlo simulations.

Results: The CRFs in this study show reduced model uncertainty compared with previous CRFs in all endpoints. The nonlinear CRFs produce more than doubled global estimates on average, depending on the endpoint. Overall, we assess that our CRFs can be used to provide policy analysis of air pollution impacts at the global scale. It is however important to note that improvement of CRFs requires observations over a wide range of conditions, and current available literature is still limited.

Discussion: The higher estimates produced by the nonlinear CRFs indicates the possibility of a large underestimation in current assessments of the morbidity impacts attributable to air pollution. Further studies should be pursued to better constrain the CRFs studied here, and to better characterize the causal relationship between exposures to PM$_{2.5}$ and morbidity outcomes.

1. Introduction

The World Health Organization (WHO) has estimated that 4.2 million premature deaths were attributable to ambient fine particulate air pollution in year 2016,(Bai et al., 2019) with other studies reporting much larger impacts when considering the full set of noncommunicable diseases.(Beverland et al., 2012; Bowe et al., 2018) While the estimated mortality burden is unquestionably important, it is also important to estimate morbidity, such as incidence of air-pollution related diseases, hospital admissions (HA), emergency room visits (ERV), and lost

---

* Corresponding author at: The Earth Institute, Columbia University, New York City, NY, USA.
 E-mail address: muye.ru.work@gmail.com (M. Ru).

productivity.(Brook et al., 1997; Burnett et al., 2018) Such estimates allow for an accounting of non-fatal health impacts and their costs, for example through cost-of-illness, defined as estimates of the value of resources that are expended or foregone as a result of a health problem, such as health sector cost, decreased productivity, and the cost of pain and suffering.(Burnett et al., 2014) Morbidity estimate thus could enable a more comprehensive assessment of the cost of air pollution to inform policy analysis.

The estimation of both mortality and morbidity burdens associated with air pollution is based on concentration–response functions (CRFs). CRFs statistically estimate the relationship between exposure to pollutants and health outcomes, with concentrations of pollutants acting as a surrogate for outdoor exposure. The CRFs between long-term exposure to ambient air pollution and mortality have been extensively studied, systematically documented and regularly updated in efforts such as the Global Burden of Disease studies(Cai et al., 2014) as well as in many peer-reviewed papers. (Beverland et al., 2012; César and Nascimento, 2018; Chen et al., 2013) In contrast, CRFs for morbidity endpoints have been less studied. For that reason, we focus our study on morbidity, in particular on impacts associated with short-term exposures to particulate matter with an aerodynamic diameter less than or equal to 2.5 microns ($PM_{2.5}$) as there are more data available for these than other impacts.

A major limitation in commonly-used $PM_{2.5}$ CRFs for most morbidity endpoints is that they primarily rely on studies conducted in Europe and North America.(Brook et al., 1997; Burnett et al., 2018; DeFlorio-Barker et al., 2019) This limits their use for other regions where exposure levels can be much higher. To enable a more accurate worldwide estimation of morbidity, we conduct a *meta*-analysis of recent epidemiological studies globally for $PM_{2.5}$-based morbidity endpoints. We chose the morbidity endpoints included in this study based on the CaRBonH project, the most recent morbidity assessment from the WHO.(Burnett et al., 2018) The endpoints we focused on in our systematic review thus included all cardiovascular HA, all respiratory HA, asthma HA and ERV, along with the outcomes that stem from morbidity, such as lost work days, respiratory restricted activity days (RRAD), and child bronchitis symptom days. All the endpoints above have been evaluated as having either a "causal relationship" or "likely to be a causal relationship" based on the review of evidence conducted by a group of experts in the Integrated Science Assessment (ISA) for particulate matter organized by the US EPA.(Dong et al., 2020) They are therefore also included in the BenMAP-CE tool developed by the US EPA.(DeFlorio-Barker et al., 2019).

Using the data collected in our *meta*-analysis, we derived new CRFs covering a large range of $PM_{2.5}$ concentrations. Furthermore, in addition to using a log-linear model as in previous morbidity CRFs, we also defined a nonlinear functional form to enable more flexibility over the large range of concentrations. Previous work has shown CRFs for mortality related to $PM_{2.5}$ exhibit a strong nonlinearity. (Burnett et al., 2018; Burnett et al., 2014; Strak et al., 2021) Among the morbidity studies in our review, Erbas et al. (Erbas et al., 2005) also reported presence of nonlinearity within the study.(Feng et al., 2019) Hence here we also examine nonlinearity in the CRFs for morbidity. Specifically, previous work deriving CRFs for mortality provides a framework for the nonlinear functional form.(Beverland et al., 2012) We adapt that functional form here and constrained the CRF shape parameters using their "study-level" modeling approach, such that the average effect from each study is used as input (as opposed to the "subject-level" functional form, which requires data for each person in the study that is not available). We computed CRFs using log-linear and nonlinear functional forms to explore the underlying strengths and limitations of both approaches. We then conducted sensitivity analysis of the CRFs to any individual study through one-at-a-time withdrawal from the entire set of studies.

This paper is organized as follows: in the Methods section, we describe our methodology to identify the studies of interest, from which we extract data to construct new CRFs. In the Results section, we present results and provide an assessment of model uncertainty. In the

Discussion section, the limitations of our analysis are considered and conclusions are drawn, in addition to identifying new areas of development.

2. Methods

We used a three-step methodology to construct the morbidity CRFs for a variety of end-points: 1) we systematically reviewed peer-reviewed publications documenting specific morbidity impacts related to $PM_{2.5}$, 2) we conducted a *meta*-analysis of the reviewed studies and estimated the various CRFs, using both log-linear and nonlinear functional forms, and 3) we performed an extensive analysis of model uncertainty.

2.1. Systematic review and eligibility criteria

As noted, the endpoints included all cardiovascular HA, all respiratory HA, asthma HA and ERV, along with the outcomes that stem from morbidity, such as lost work days, respiratory restricted activity days (RRAD), and child bronchitis symptom days, as in CaRBonH. (Burnett et al., 2018) For each endpoint, we performed a systematic review of available papers. Our search strategy followed the Preferred Reporting Items for Systematic Reviews and Meta-Analyses (PRISMA) process, as shown in the flow diagram in Figs. S1-S4. There were three steps in our search strategy. The first step was a literature search for each morbidity endpoint listed above in the PubMed database (https://pubmed.ncbi.nlm.nih.gov), using the search terms in Table S1 The final search date was June 30th, 2020.

The second step was to only include the studies which reported estimated 95% confidence intervals (CIs) on the relationship between 24 h $PM_{2.5}$ (or PM_{10}, see below for our conversion to risk estimates of the equivalent $PM_{2.5}$ component of PM_{10}) exposures and the endpoints at multiple lag days. That is, we only included studies that reported an originally-developed relative risk (RR), odds ratio (OR), hazard ratio (HR), percent increase in risk, or regression coefficients, as risk estimates. The RR, OR, and HR have been used interchangeably when extracting data from the literature.

As a third step, we assessed the eligibility of each study based on our inclusion/exclusion criteria below and conducted conversion when needed. Table S2 presented a complete list of studies we included in the *meta*-analysis, including the time and location, age group, sample size, risk estimates and their uncertainty range, the range of $PM_{2.5}$ concentrations (including those transformed from PM_{10}), the lags selected, and rationale for the selection(s) from studies where multiple risk estimates were extracted. Studies sometimes reported multiple independent risk estimates, such as for different regions, exposure ranges, or age groups. These risk estimates were used as independent data inputs when possible (see Discussion). Our specific inclusion/exclusion and conversion criteria are explained in Table 1. Funnel plots are used to evaluate the potential presence of publication bias.

2.2. Data extraction

We extracted from each study *i* the risk estimates, such as RR, OR, HR, percent increase, or effect estimates (β_i as in Eq. (1)), and corresponding confidence intervals:

$$RR = \exp(\beta_i \Delta x) \tag{1}$$

where Δx was the exposure increment reported in the study, typically 10 μg/m³. After excluding outliers, we examined if there was evidence for distinct CRFs for each age group or whether a single CRF applies to all age groups. For asthma ERV and asthma HA, we found several studies focusing on children while others reported results for the all-age population. For cardiovascular HA, some studies focused on the post-65 population while others were for all ages. In cases where different age groups were presented, we conducted a Student's *t*-test analysis on the

Table 1
Inclusion/exclusion criteria for the *meta*-analysis.

Focus	Criteria
Scope	We focused on studies examining all cardiovascular (codes 390–459 based on the International Classification of Diseases, Ninth Revision (ICD-9), or I00-I99 based on the Tenth Revision (ICD-10)) and all respiratory (codes 460–519 in ICD-9 or codes J00-99 in ICD-10) HA, but not those breaking down to study specific causes within the above groups, because our primary goal was to assess the total morbidity impacts. However, we decided to study both asthma HA and all-respiratory HA separately since we noticed that the risk estimates of asthma HA were generally higher than that of all respiratory HA. (DeFlorio-Barker et al., 2019; Wong et al., 1999) This way, users of these CRFs could estimate all-respiratory HA and asthma HA respectively, depending on the need.
Exposure types	We have identified two classes of studies: studies that directly focused on PM$_{2.5}$ concentrations and studies that reported risk estimates for PM$_{10}$. There is growing understanding that fine particles are the most harmful for human health among the entire size distribution. (U.S. Environmental Protection Agency, 2022) However, we include both to increase the size of the evidence base. This is justifiable because there is a relatively high correlation between PM$_{2.5}$ and PM$_{10}$ (i.e., mostly above 70% (Zhou et al., 2016; Brook et al., 1997)). In our study, whenever necessary, we calculate the equivalent PM$_{2.5}$ component among PM$_{10}$ to convert the risk estimates for PM$_{10}$ to PM$_{2.5}$. This was performed using the results of a chemistry-climate model GISS-E2.1-G developed at NASA. (Kelley et al., 2020) From those results, we summed the PM$_{2.5}$ concentration and the PM$_{10}$ concentration of the near-surface aerosol mass-concentration, and calculated the average ratios at the country-level. For example, since the average ratio of PM$_{2.5}$ and PM$_{10}$ over the US was estimated to be 0.60, based on our model results, the reported risk estimates per 10 mg/m^3 PM$_{10}$ were converted to the risk estimates per 6 mg/m^3 PM$_{2.5}$.
Lags	Among the multiple lag (observation of increased risk lagging the 24-hour average PM$_{2.5}$ observation) days examined in each study, we only used the largest risk estimate, regardless of the lag. This practice is both for simplicity and for taking into consideration the potentially different response time in medical resources, such as emergency room availability or available beds in hospitals. When the largest risk estimate reported is for a cumulative period, such as lag 0–2 or 0–6, we select this cumulative period as the chosen lag.
Type of models	We only used risk estimates from single-pollutant models in this study, not including risk estimates derived from multiple-pollutant models, such as ozone or NO$_2$.
Extreme values	When all eligible studies were obtained, we then screened for extreme values among the risk estimates reported from each study. We excluded risk estimates that fall outside of Q1 - 3*IQR and Q3 + 3*IQR, where Q1 and Q3 indicates the 25th and 75th percentiles of the distribution of all the risk estimates from studies, and IQR indicated the interquartile range between 25th and 75th percentiles. This was done to avoid the sensitivity of CRFs to certain studies with extreme values.

results in the *meta*-analysis to compare the mean of the two distributions of morbidity effects (Table S3). If a significant (p-value < 0.10) difference was detected between age groups, we estimated CRFs for different age groups separately. For respiratory HA, three age groups were presented, so we used a one-way ANOVA to compare the means of the three groups.

We also extracted the 5th and 95th percentiles of PM concentrations (either PM$_{10}$ or PM$_{2.5}$) in each study. Using the 5th and 95th percentiles avoided the influence of extreme levels of PM concentrations. When those percentiles were not directly reported, we followed the approach in Appendix 1.1 to estimate the ranges of concentrations.

2.3. Derivation of concentration-response functions

The log-linear concentration–response model can be expressed as:

$$RR = \exp(\beta x) \tag{2}$$

where β is the coefficient of the concentration–response effect and x is the exposure to PM$_{2.5}$. In usual cases, x would be represented as

$PM_{2.5} - cf$, where *cf* represents the counterfactual level, usually defined as the 5th percentiles or the minimum of each study. In our study, however, either the 5th percentiles or the minimum of each study turned out to be below 1 ug/m^3 for all endpoints. We therefore did not consider the existence of meaningful counterfactual levels for the morbidity endpoints examined here. As such, Eq. (2) is essentially the same as Eq. (1), where Δx is x.

We also used a nonlinear function with additional parameters (α, μ, τ) to allow for the curvature and shape of the CRF to change across the range of exposures. This modeling approach was originally developed for subject-level modeling,(Ferreira et al., 2016) and was developed into a common model for cohort-level derivation of CRF for the global mortality(Beverland et al., 2012) and morbidity in Canada.(Heymann, 2009) According to this approach, the exposure-outcome association (RR) is characterized according to:

$$RR = \exp(\theta T(x)) \tag{3}$$

where,

$$T(x) = \ln(1 + x/\alpha)\omega(x) \tag{4}$$

$$\omega(x) = 1/(1 + \exp\{-(x - \mu)/(\tau r)\}) \tag{5}$$

where x is as in Eq. (2); θ is the regression coefficient, estimated while specifying different values of (α, μ, τ); r is the exposure range, defined as the difference between the lowest 5th percentile and the highest 95th percentile in exposure ranges among all studies; and $\omega(x)$ is a weighting function, where μ controls the shape of ω, and τ controls its curvature. The log function in Eq. (5) represents the natural logarithm. The nonlinear regression was conducted using the nlm package in R 4.1.0, and the details are discussed in Appendix 1.2.

2.4. Model fitting and estimation of uncertainties in the CRFs

To obtain synthesized CRFs and quantify their model uncertainty, we implemented a two-step approach. First, for each of the log-linear and nonlinear CRFs, we computed an ensemble of model fits by bootstrapping the risk estimates reported from each study, in order to create a statistical representation of its full distribution. Specifically, we randomly resampled (10,000 times) the risk estimates (β_i in Eq. (1)) from each study, using a normal distribution with the mean and standard deviations obtained from each study (Fig. S5). Then by using $\Delta x_{95th-5th}$ and Eq. (1), we created a set of 10,000 RR values for each study. As such, for an endpoint with effect estimates from n studies ($i = 1, 2, \ldots, n$), we obtained 10,000 set of input data, each including n pairs of ($\Delta x_{95th-5th,i}$, RR_i). These were essentially n pairs of independent and dependent variables used for model-fitting.

As a second step, we implemented the model-fitting approaches described above using the n pairs of data in each of 10,000 sets, to obtain 10,000 estimates of β for the log-linear CRF and 10,000 estimates of $(\theta, \alpha, \mu, \tau)$ for the nonlinear CRF. To measure "goodness of fit", we calculated the log-likelihood from each estimate of both log-linear and nonlinear CRF. We then used the mean of the estimates of β and θ, while taking the "mode" (the most frequent result) for parameters α, μ, and τ, as our central CRFs (Tables 2-3).

We then generated the range of model uncertainty for the CRFs. For each level of PM$_{2.5}$, we performed a Monte-Carlo simulation based on a normal distribution using the mean and standard deviation of β and θ from above to make 10,000 predictions of RR using Eqs. (2) and (4). We then found the 5th and 95th percentiles of those RR estimates to plot the uncertainty ranges in Fig. 1. This Monte-Carlo step was implemented using R programming as described in Appendix 2.

2.5. Computation of morbidity

We used the RR (see Eq. (2)) to derive attributable fractions (AF) as:

Table 2

Summary of regression coefficients and log-likelihood of log-linear[1] concentration response functions (CRFs).

Endpoint	Age group	Number of observations extracted	Relative risk[1] (RR, 10 µg/m^3)	95% confidence interval of RR	Log-likelihood (LL)	Full exposure ranges from observations (µg/m^3)
Asthma emergency room visits	All ages	26	1.043	(1.026, 1.062)	−28	0–184
Asthma hospital admission	All ages	17	1.014	(1.008, 1.020)	−8	0–399
Asthma hospital admission	Children (below 20)	16	1.048	(1.024, 1.072)	−4	0–133
Cardiovascular hospital admission	All ages	28	1.010	(1.006, 1.014)	10	0–268
Cardiovascular hospital admission	Post 65	18	1.0126[2]	(1.0095, 1.0158)	40	0–112
Respiratory hospital admission	All ages	46	1.0135	(1.0104, 1.0166)	20	0–380

Note [1]. For log-linear functions, $Ln(RR) = bx$, $x = 10$ µg/m^3 for this table.
Note [2]. For cardiovascular hospital admission for post-65 population and respiratory hospital admission for all-age population, we have four decimal places instead of 3, to provide more details that distinguishes the two endpoints, as rounding up to 3 decimal places would lead to the same numbers.

Table 3

Summary of regression coefficients, parameters, and log-likelihood of nonlinear concentration response functions (CRFs).

Endpoint	Age group	Number of observations extracted	Relative risk[1] (RR, 10 µg/m^3)	Confidence interval of RR (approximated[2])	a	μ	τ	range, r	Log-likelihood (LL)	Full exposure ranges from observations (µg/m^3)
Asthma emergency room visits	All ages	26	1.115	(1.069, 1.164)	1	19.7	0.1	184	−7	0–184
Asthma hospital admission	All age	17	1.068	(1.037, 1.099)	1.5	32.6	0.1	399	2	0–399
Asthma hospital admission	Children (below 20)	16	1.157	(1.063, 1.259)	1.4	NA[3]	NA	NA	1	0–133
Cardiovascular hospital admission	All ages	28	1.050	(1.033, 1.067)	1.1	1.6	0.1	268	18	0–268
Cardiovascular hospital admission	Post 65	18	1.019	(1.005, 1.032)	3	21.7	0.2	112	41	0–112
Respiratory hospital admission	All ages	46	1.037	(1.024, 1.050)	5.6	9.0	0.1	380	32	0–380

Note:
[1]. For nonlinear functions, $Ln(RR) = \theta \ln(x/\alpha + 1)w(x)$, $x = 10$ µg/m^3 for this table.
[2]. Because the confidence intervals of nonlinear CRFs are depend on x, they are reported as an approximation when $x = 10$ µg/m^3 in this table.
[3]. The μ, τ, and r, are NA for this endpoint. This means that the optimized result from our regression is a function where $\omega(x) = 1/(1 + \exp(-x))$.

$$AF = 1 - 1/RR \tag{6}$$

where AF was the fraction of total morbidity attributed to a specific PM$_{2.5}$ exposure, such that:

$$\Delta Morbidity = y_0 \times AF \times Population \tag{7}$$

where y_0 was the baseline morbidity rate of each endpoint, and population was the total population in the age groups relevant to the morbidity endpoint of interest. Δ Morbidity was the excess morbidity that was associated with PM$_{2.5}$ exposure. For simplicity, we assumed all persons were equally exposed to the same level of ambient air pollution at a given location.

We calculated RR by applying both functional forms in Eq. (2) and (3) to a 0.5 by 0.5 global estimates of PM$_{2.5}$ exposure, obtained from van Donkelaar et al. (Van Donkelaar et al., 2018).(Holland, 2014) To compare the impacts of the two functional forms, we calculated the ratio K$_{nl/ll}$ between morbidity estimates from the nonlinear CRFs and the log-linear CRFs for each grid point. Note that, by definition, K$_{nl/ll}$ was independent of both y_0 and population. When K$_{nl/ll}$ was greater than 1, the nonlinear CRFs produce higher estimates. When it was between 0 and 1, the log-linear CRFs produced higher estimates.

Finally, we calculated the ratio of AF when using an "annual average" exposure approach versus using a "daily sum" approach, which we called R$_{a/d}$. In a linear case, the "annual average" approach was equivalent to the "daily sum" approach, and R$_{a/d}$ was 1 when above the counterfactual levels. The log-linear CRFs can closely approximate linear functions, especially over narrow ranges of PM$_{2.5}$. The nonlinear CRFs, however, can deviate more from a linear function form, and thus can have a R$_{a/d}$ further from 1. The extent of deviation depends on the distribution of daily exposures over the year, and on the shape of the specific CRFs.

3. Results

3.1. Meta-analysis and CRF

Our systematic review included 93 studies in total, which are documented in detail in Table S2. A summary of the main features is shown in Table 4. Since some studies reported multiple independent risk estimates, we ended up extracting 160 risk estimates from them. These multiple risk estimates in a single study could be for different morbidity endpoints, exposure ranges, age-groups, or time. Among the 160 risk
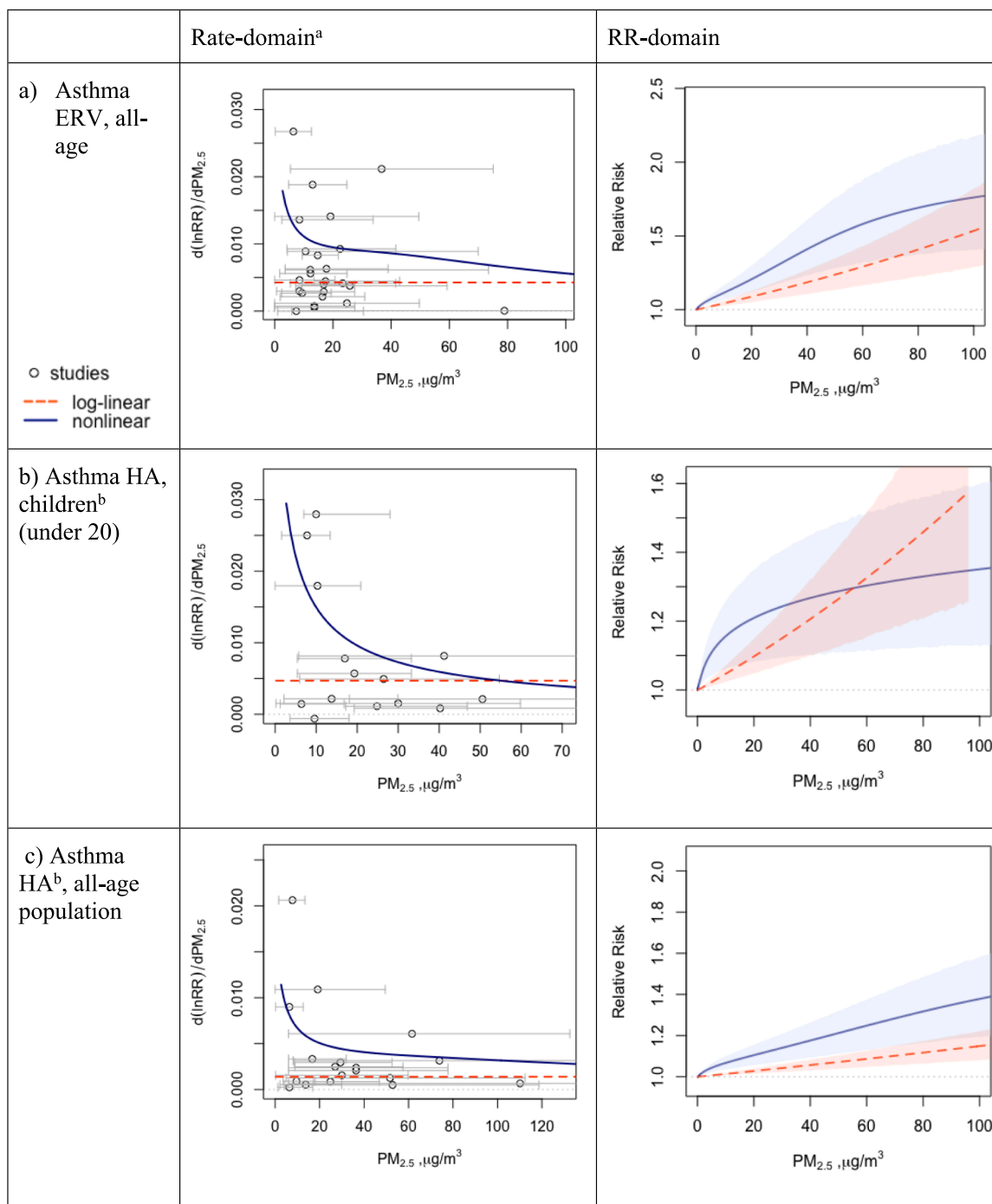
Fig. 1. Concentration-response functions (CRF) in log-linear and nonlinear forms for each morbidity endpoint. The rate-domain shows the comparison to the original observations from the meta-analysis, where the horizontal bars indicate the 5th to 95th contrast used to determine the risk estimates in the original studies. The relative risk (RR)-domain shows the changes of RR in response to $PM_{2.5}$ exposure, where the shaded areas indicate 95% confidence intervals. Numeric data for the figures were included in Table S2. Note:[a] in the rate domain, the curves depict $\Delta RR / \Delta x$. In the RR-domain, the dashed line corresponds to Eq. (2), $RR = exp(bx)$; whereas the solid lines correspond to Eq. (3) $RR = exp(\theta ln(x+1)\omega(x))$.

estimates, 34% were from North America, 27% from Asia, and 20% from Europe. In addition, we also had 11% from Oceania, 6% from South America, and 1% from the Middle East. As such, our study had a relatively good geographic coverage of evidence. Funnel plots for each morbidity endpoint are presented in Fig. S6, indicating potential presence of publication bias in the *meta*-analysis, especially for asthma EV, cardiovascular HA for all-age population, and respiratory HA for all-age population. This can be a limitation of this study (see Discussion).

We show in Fig. 1 the log-linear and nonlinear CRFs for each endpoint considered. The left-panel presents the rate of change of RR (i. e., $d(lnRR)/dx$ as derived from Eq. (2) and (4)) as a function of exposure. We show the horizontal ranges associated with each data point, representing the range of concentrations over which the effect was identified in a particular study. In the right panel of Fig. 1, we show how the RR changes with exposure, which displays how CRFs link risks to exposures, referred to as the "RR-domain" hereafter. The nonlinear CRFs had more

d) Cardiovascular HA, all-age population

e) Cardiovascular HA, elderly (65+) population

f) Respiratory HA[b], all age

Fig. 1. (*continued*).

3.1.1. Respiratory morbidity outcomes

3.1.1.1. Asthma. Most ERV studies were conducted in cities in Europe and North America, with only three exceptions from Australia, Korea, and China. HA studies had a more globalized geographical coverage, with about half conducted in Asia. There was no strong evidence of a meaningful counterfactual level for the asthma-related endpoints and age groups. In general, asthma ERV showed a shorter lag than asthma HA. For ERV, all but three studies included in the *meta*-analysis

freedom to adapt to the shape of the input data, thus unsurprisingly have a better fit to the empirical data, indicated by larger loglikelihood values. Yet, the goodness of fit is not the only criteria when selecting which CRFs to use. Rather, the specific goals when applying the CRFs should guide model selection (see Discussion).

indicated a relatively short lag between 0 and 3 days (Table S2), and six were at lag 0. For HA, meanwhile, the chosen lags were mostly in the range of 0–5 days, indicating the HA effect may take place with a slightly longer lag than the ERV effect.

For the asthma emergency room visits, a Student's *t*-test did not indicate a significant difference between the risk estimates for children from those for adults (Table S3, Fig. S7), yet it did indicate a higher significance level (narrower error bars) for children. We used all observations to construct a CRF that applied to the all-age population (Fig. 1-a). In the rate-domain, for both child and all-age asthma ERV, we found significant variance in the risk estimate β_i among studies at concentration levels below 20 μg/m³. As a result of the root mean square error (RMSE) minimization of the fitting process, the nonlinear functional form predicts relatively higher (supra-linear) risk estimates than the linear case, especially for concentrations below 20 μg/m³. Since this

Table 4
Summary for each endpoint of the *meta*-analysis results.

Endpoint	# studies	# observations	Outliers identified
Asthma HA	24	33	0
Asthma ER	33	48	0
All-respiratory HA	35	48	3[1]
Cardiovascular	37	48	2[2]
Work days	1	1	0
RRAD	3	3	0
Children bronchitis	2	2	0

[1] The three observations identified were shown in Fig. S8 (Machin et al., 2019; César and Nascimento, 2018; Silva et al., 2013), Further sensitivity analysis on inclusion/exclusion of these outliers are discussed in 1. Potential source of bias in the derived CRFs in Discussion.

[2] The two observations identified were shown in Fig. S9 (Ferreira et al., 2016; Soleimani et al., 2019), Further sensitivity analysis on inclusion/exclusion of these outliers are discussed in 1. Potential source of bias in the derived CRFs in Discussion.

behavior occurs in most of the morbidity endpoints we study here, we do not discuss this point again in the endpoints below.

For the asthma hospital admissions, 16 of the 33 observations were focused on children, defined as below-20. Children's age groupings varied across studies (details in Table S2), and below-20 encompassed the ranges of different studies. In addition, thirteen studies were for all-age population, and four studies were for below-65 population. We find that the post-65 and below-65 studies have a similar mean risk estimate, and all of them appear to be within the range of the estimates for the all-age population (Fig. S8). We therefore merged below-65 and post-65 observations with the set of all-age observations and examined their difference from observations for children. A Student's *t*-test suggested a significant difference in β between the child and adult age groups, however (Table S3). We therefore estimated CRFs for children and all ages separately (Fig. 1-b, c). Both nonlinear and log-linear models predicted a larger effect, and therefore higher RR, for children.

3.1.1.2. Hospital admissions for all-respiratory diseases. In addition to asthma HA, we also estimated the CRF for all-respiratory HA. Amongst the studies, 6 were focused on children, 18 on elderly people, and the rest on the all-age population. One-way ANOVA and box plots showed no significant differences among these three groups (Table S3, Fig. S9). We therefore constructed the CRFs for the all-age population using all the data available. 29 of the 48 observations reported the highest risk estimate between 0 and 3 days, yet there were also studies that found the highest risk estimate at an extended lag of 11 days,(Kelley et al., 2020) 14 days,(Kim et al., 2012) and 0–14 days.(Kowalska et al., 2019).

3.1.2. Cardiovascular morbidity outcomes

Among the observations included in the *meta*-analysis for cardiovascular endpoints, 18 were focused on elderly people (post-65), and 28 were focused on the all-age population. We found that the mean effect estimate for the post-65 group was significantly lower than the all-age group (Table S3, Fig. S10). We thus estimated CRFs for these two groups separately (Fig. 1-d, e). We used a counterfactual level of 0. Compared to the other endpoints, cardiovascular HA had relatively short lags. 26 out of the 46 observations reported the highest risk estimate at either 0 or 0–1 lags. All reported lags were within 0–6 days.

3.1.2.1. Work days lost. The $PM_{2.5}$ effect on work days lost was only studied for US adults over 1976–1981.(McConnell et al., 1999) The mean effect was RR = 1.05 (confidence interval of 1.04–1.05) per 10 μg/m^3 $PM_{2.5}$, calculated as the average across years weighted by the variance of each year's effect.(DeFlorio-Barker et al., 2019) This study focused on a 2-week lagging period.

3.1.2.2. Respiratory restricted activity days. RRAD was a broader

category than work days lost, reflecting general activity reduction, but not limited to work loss. Our systematic review resulted in only three studies which examined the linkage between RRAD and exposures to fine particles: Willers et al. (Willers et al., 2013); Ostro (Ostro, 1989), and Ostro and Rothschild (Ostro and Rothschild, 1989)0.22,23,Murray et al., 2020 We discussed and compared these results, along with some other related studies on absenteeism and exposure to PM pollution in Discussion and Appendix 3.

3.1.2.3. Child bronchitis symptom days. Bronchitis symptoms among children were often related to lower respiratory infections. Our systematic review resulted in two studies, conducted in Chile(Ostro, 1987) and the US(Ostro, 1989). Among these studies, Pino et al. (2014) focused on infants below 1-year,(Ostro, 1987) finding a RR = 1.05 (1.00, 1.09) at a 1-day lag for prevalence of bronchitis per 10 μg/m^3 increase of $PM_{2.5}$. McConnell et al. (McConnell et al., 1999) studied the risk for children between 10 and 15 years old,(Ostro, 1989) and found that children with asthma or wheeze had significantly higher risk of bronchitis at the same day of exposure. Based on the fractions of children with asthma and wheeze in the study, the equivalent RR for bronchitis was 1.13 (0.90, 1.46) per 10 μg/m^3 $PM_{2.5}$ at lag 0 for the population of children in the study.

3.1.3. Other outcomes that stem from morbidity

For completeness, we have included here a brief discussion of work days lost, respiratory restricted activity days (RRAD), and child bronchitis symptom days, since they all have been discussed in regulatory impact assessments such as HRAPIE(Machin et al., 2019) and CaRBonH. (Burnett et al., 2018) However, because of the limited number of studies, we only provided a narrative discussion of these studies, without computing a CRF because such a CRF may not be of the same level of confidence as those of the other endpoints. We however included an exploratory CRF for RRAD based on the currently available data in Discussion. We note that future epidemiological evidence on these endpoints would be especially important to better characterize the shape of their CRFs.

3.2. Sensitivity to excluding individual studies used to derive the CRFs

In this analysis, we excluded each study separately and iterated steps 1 and 2 in Fig. 1 to create estimates for the alternative CRF. We then compared the fitted coefficients and parameters from each of the one-removal-at-a-time simulations to those from the main results to evaluate if the CRFs were sensitive to individual studies. The sensitivity associated with the exclusion of individual studies is presented in Fig. S11. We find that, for the CRFs presented in Fig. 1, exclusion of individual studies does not cause significant deviations from the main models. The ranges of model uncertainty (i.e., width of the curves in Fig. S11) still largely overlap. The exceptions are two of the log-linear CRFs. In one, there was a 144% change in the risk estimate (β = 0.0084) for asthma ERV when excluding Feng et al. (Feng et al., 2019). (Ostro and Rothschild, 1989) The other one was an 84% change in the risk estimate (β = 0.0024) for asthma HA when excluding Cai et al. (Cai et al., 2014).(Pino et al., 2004) As such, the log-linear models for these two endpoints are less robust than others. Table S4 and Fig. S12 (excluding the above two extreme cases for better visualization) show the ranges of the difference in the mean estimates as percentage departures from the main model. In general, when excluding the two extreme cases for log-linear CRFs, the differences seen in the one-removal-at-a-time test were comparable between log-linear and nonlinear models, and were within 20% of the estimates from the respective main models.

3.3. Application of the CRF functional forms

To evaluate the impacts of using different functional forms, we apply both to global PM$_{2.5}$ concentration estimates at a resolution 0.5° by 0.5°, (Machin et al., 2019) and computed the respective AF (Fig. S13) and their ratio K$_{nl/ll}$ (Fig. 2). Given that most regions did not have a high average PM$_{2.5}$ concentration, the morbidity estimates using the nonlinear CRFs lead to higher estimates in most regions (Fig. 2 and Fig. S13), owing to the supra-linear behavior at low PM$_{2.5}$. Furthermore, due to their concavity, we find that the nonlinear functions generally led to higher morbidity burdens across different morbidity endpoints. Overall, the spatial patterns in Fig. 2 indicates that the regions with very low (less than 5 μg/m^3) PM$_{2.5}$ concentrations are most sensitive to the choice of functional forms. This implies that our knowledge of the exposure response function in low-concentration regions is still limited, and caution should be used when evaluating these impacts in these regions. We further discuss this sensitivity in Discussion. However, these regions are usually not highly populated. By contrast, most areas with large populations, such as East and South Asia, Europe, and large cities in the Americas, appear to have relatively lower sensitivity, with K$_{nl/ll}$ usually ranging between 1 and 3. On a global basis, this still indicates a considerable difference in morbidity estimates given the large populations in those regions. Specifically, everything else being equal, the use of the nonlinear CRFs would lead on average to more than doubled total estimates in all the analyzed morbidity endpoints associated with PM$_{2.5}$ exposures.

4. Discussion

Using the data collected in our *meta*-analysis, we have derived new CRFs covering an extended range of PM$_{2.5}$ concentrations for four morbidity endpoints and discussed the evidence for three additional endpoints stemming from morbidity. We have also presented the model uncertainty associated with the CRFs and evaluated the application of both the non-linear and loglinear CRFs.

The possible presence of a potential selection bias can be found in the asymmetry of Fig. S6. Theoretically, this could potentially exaggerate the morbidity impacts suggested by the CRFs. However, as the asymmetry in the funnel plots is limited, the potential magnitude of bias should be small except perhaps in the case of Asthma HA for children.

In this work, several choices we made are potential sources of bias. Here we discuss the reasons for making these choices and their potential impacts.

Firstly, in our data collection, we selected the lag between exposure and impact with the highest risk estimate; this is both for simplicity and to allow for variations in the time it takes for the largest effects to occur. Theoretically this could cause our estimates to lie at the higher end. Yet this effect should be quite limited because all the CRFs are tested against the bias from a single study using the bootstrapping method documented in *the Subsection* 3 *(Model fitting and estimation of uncertainties in the CRFs)* of *Methods*.

Secondly, the data we extracted in this study are considered under the single-pollutant model. This is because our primary goal was to expand the evidence-based analysis globally, and single-pollutant models are the most commonly reported. However, the single-pollutant approach provides limited insights regarding co-exposures and may lead to different risk estimates than when considering co-exposures, for example to NO$_x$ and O$_3$. Usually, the single-pollutant approach leads to a slightly larger risk estimate than a multi-pollutant approach. However, it can also be the opposite. Without further knowledge on the impacts of co-exposures on the morbidity outcomes examined, it is impossible to determine the specific impacts of taking a single-pollutant approach. Further studies should continue to review and examine the evidence using multi-pollutant models. In addition, we have also tested the sensitivity when not removing the extreme values as outliers, and showed that could cause significant sensivity in the one-at-

a-time removal practice. Detailed comparisons are shown in Appendix 4.

Thirdly, in our data collection for the *meta*-analysis, we treated multiple risk estimates from a single study as independent input data points in regression. This could mean that errors among certain data points are correlated, instead of completely independent. However, the impacts of this treatment on our CRF results should be very limited. Because correlated error terms could cause underestimation of standard deviations, therefore the independence assumption will influence the estimation of the confidence intervals. But in our study, the confidence intervals, or model uncertainty, was obtained from model spreads based on simulations of resampled data. As such, the CRF results should not be biased due to this issue. Yet we realize that there can be more advanced statistical approach to tackle this issue, such as mixed-effect models.

Lastly, we didn't consider variation in toxicity of different components of PM, though each study in the *meta*-analysis could have had a different chemical profile of PM$_{2.5}$. Further evaluation of the composition of PM$_{2.5}$ could be valuable when more evidence becomes available. We also did not address the impacts of indoor exposures on these CRFs. Specifically, several studies have shown that the deviation of total exposures from ambient PM$_{2.5}$ can significantly impact risk estimates, leading to underestimation of the total effects of PM$_{2.5}$ exposures. (Dong et al., 2020; US EPA)

We compare them with previously published CRFs to understand the impacts of the updated CRFs derived in this paper. These include the WHO CRFs based on the HRAPIE (WHO, 2013) and CaRBonH studies, (Spadaro et al., 2018) mainly focused on Europe. In addition, the US EPA developed the BenMAP-CE tool, (U.S. Environmental Protection Agency, 2015) based on epidemiological studies conducted in the US and Canada. Notably, Fig. S14 displays the CRFs from the WHO, or if unavailable, from BenMAP-CE. We emphasize the WHO's CRFs as they are a synthesis of multiple studies and are therefore more directly comparable to our results. We observe that our CRFs exhibit greatly reduced ranges of model uncertainty. There are two main reasons for this behavior. First, due to the global focus of our study, we included more epidemiological studies in our evidence base than the previous CRFs, therefore constraining the CRFs more firmly. Second, the confidence intervals in our study are developed using a bootstrapping-based simulation approach, which generate confidence intervals from resamples as per central limit theorem, instead of a traditional statistical approach in previous systematic review and *meta*-analyses. We find that our central estimates using log-linear CRFs are higher than the WHO estimates for post-65 cardiovascular HA (as post-65 were included in the all-age cardiovascular HA calculation using the WHO approach), but lower for respiratory HA, and about the same for all-age cardiovascular HA. When compared to BenMAP-CE, our log-linear results lead to lower estimates in all-age asthma HA, but higher estimates for childhood asthma HA, and similar values for asthma ERV. Our nonlinear CRFs, by contrast, generated different magnitudes and spatial patterns, as shown in Fig. S13 and discussed in Section 3 in Results, due to the fundamental difference in functional forms.

It is important to note that both the previously published CRFs and the new ones we present describe the associations between morbidity outcomes and PM$_{2.5}$ exposures. In this sense, the fact that our work included expanded evidence worldwide and thus significantly reduced model uncertainty does not indicate an advance in our understanding of causality. However, the fact that our results show statistically robust estimates of RR larger than 1 over the exposure ranges, considering all the published evidence, there is a strong indication that the PM2.5 is responsible for the increase in the morbidity outcomes. Nonetheless, as we showed in Results, this can be influenced by publication bias, and therefore further research to better understand the causality is still needed.

In addition, we discuss several other important considerations in the understanding and application of CRFs, including the nonlinearity in the CRFs, the limitations in our understanding in CRFs for RRAD, and the time dimension in application of CRFs for short-term exposures:

Asthma hospital admissions for all-age population

Asthma hospital admissions for children
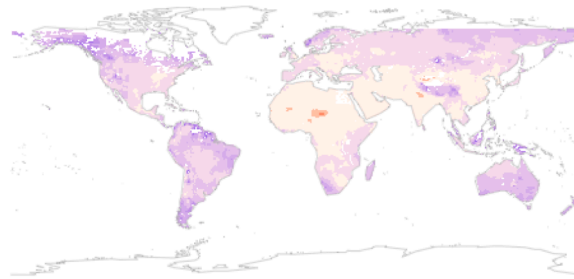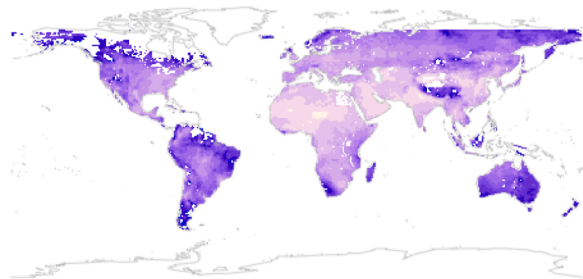
Mean $K_{nl/ll}$ =

Mean $K_{nl/ll}$ =

Asthma emergency room visit

Respiratory hospital admissions
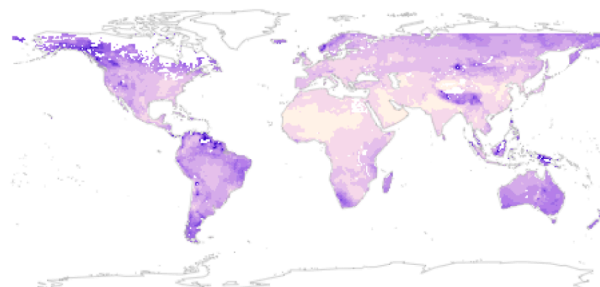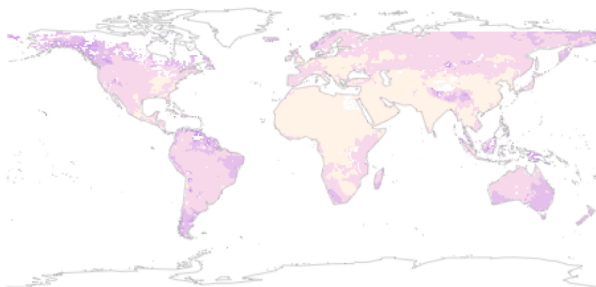
Mean $K_{nl/ll}$ =

Mean $K_{nl/ll}$ =

Below-65 cardiovascular hospital admissions

Post-65 cardiovascular hospital admissions
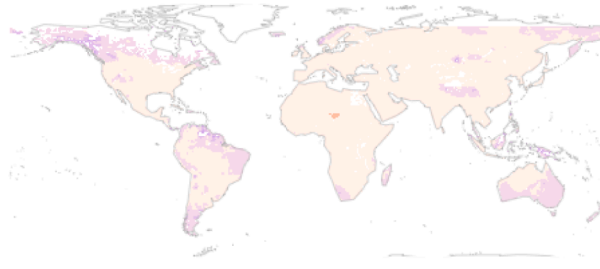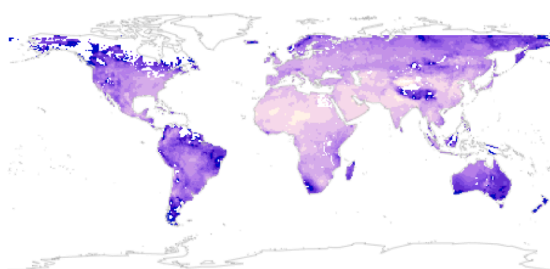
Mean $K_{nl/ll}$ =

Mean $K_{nl/ll}$ =
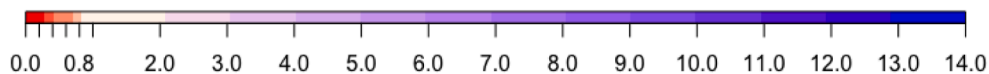
Fig. 2. Ratios of morbidity estimates with nonlinear concentration–response functions (CRFs) over with log-linear CRFs ($K_{nl/ll}$). Ratios between 0.00 and –1.00 are where the log-linear CRFs produce a higher estimate, while ratios above 1.00 are where nonlinear CRFs produce higher estimates. The results are calculated based on 0.5 by 0.5 annual exposures of $PM_{2.5}$ in 2015.

For multiple morbidity endpoints, our nonlinear functional form presents high nonlinearity in low PM$_{2.5}$ regions, leading to high sensitivity to the selection of the functional forms (Fig. 2). As noted previously, this indicates limited understanding in the exposure–response relationships in such low-concentration regions. A key factor is that indoor exposure plays a more important role in the exposure–response relationships in the low PM$_{2.5}$ regions. Given that it is difficult to obtain the "true" exposures (and the studies we reviewed hardly address this issue), we note that there is high uncertainty in the concentration–response relationships in low ambient PM$_{2.5}$ regions. As such, using the log-linear CRFs at low concentrations may be preferable to reduce dependence on the modeled nonlinearity.

Overall, we find that CRFs for RRAD are severely under-constrained. In Appendix 3, we documented the studies included in our systematic review for RRAD. Due to the limited evidence, we did not conduct a similar regression as done for the other endpoints. Here we discuss these CRFs in further details, as they have been included in regulatory impact assessments despite their substantial uncertainties.

As discussed in Appendix 3, both Ostro (Ostro, 1989) and Ostro and Rothschild (Ostro and Rothschild, 1989) used two-week average of PM$_{2.5}$ as their short-term exposure metric.23,24 To understand the impact of this choice, we conducted a sensitivity analysis regarding the influence of using 2-week averages instead of daily data, using daily 24 h PM$_{2.5}$ exposures from the Air Quality System of the United States Environmental Protection Agency, obtained from the Federal Land Manager Environmental Database (FED). (Chen et al., 2013) The results showed that the difference between using daily and biweekly averaged exposures is small (see Appendix 3). We thus used the reported risk estimates from these two studies in a regression to further explore the CRF. In addition, Ostro (Ostro, 1989) investigated RRAD from ambient air pollution (AAP),(Nasari et al., 2016) second hand smoke (SHS), and active smoking. This study built a linkage between RRAD and SHS or active smoking as a proxy for PM$_{2.5}$ exposure. Because the SHS PM$_{2.5}$ range was a closer approximation to AAP PM$_{2.5}$, we used this information in our analysis.(Chen et al., 2013) However, this was not the case for AS, which was often equivalent to thousands of $\mu g/m^3$ and thus far beyond ambient exposure levels. We thus only included the risk estimates for SHS in our exploration of a CRF for RRAD. The above two studies, together with Willers et al. (Willers et al., 2013);(Murray et al., 2020) were used to create the loglinear and non-linear regressions for the CRF for RRAD (Fig. S15; Table S5-6), following the same *meta*-analysis approach introduced in Methods. This exploration indicated the high potential of supra-linearity in the CRF for RRAD, thus further signifying caution should be used when evaluating the RRAD impacts. Essentially, any CRF for RRAD, including those from this study and other regulatory impact assessment, is currently severely under-constrained.

Finally, in practical applications of CRFs for short-term exposures, "annual average" approaches (using annual average PM$_{2.5}$ concentrations) are often used, instead of a "daily sum" approach (summing health impacts from daily PM$_{2.5}$ exposures), because annual PM data are usually more readily available. Yet the use of annual averages instead of daily values for PM$_{2.5}$ could cause a bias when users apply the CRFs developed here. To evaluate this potential bias, we applied both the log-linear and nonlinear CRFs developed in this study to the aforementioned daily ground monitoring PM$_{2.5}$ measurements. Our simulations suggested that the "annual average" approach led to an overestimation compared to the "daily sum" approach when using the nonlinear CRFs. We quantified the bias as being 0.1% - 1.2% for the loglinear CRFs and 1.7% - 4.9% for the nonlinear CRFs across morbidity endpoints. Details of our quantification are documented in Appendix 5.

Evaluation of the health impacts of air pollution considers both short-term and long-term effects. Morbidity outcomes of air pollution are usually examined on a short-term basis, such that policy evaluations of the total health burden of air pollution often encompass effects from long-term exposure-mortality, short-term exposure-mortality and short-term exposure-morbidity associations. However, these associations may not be completely independent from each other. Previous studies have implied the possibility of cumulative effects from multiple short-term exposures (i.e., intermittent exposures) or from increased sensitivity of population with high long-term exposures.(DeFlorio-Barker et al., 2019; Strak et al., 2021) Knowledge of the linkage between the effects of short and long-term exposures and the possible cumulative effects is important to further guide policy analysis.

Overall, by including more recent scientific evidence reported from a broader geographical range, and by allowing the CRF to be either log-linear or nonlinear, the morbidity CRFs in this paper provide significant updates to previous estimates of the morbidity burden associated with PM$_{2.5}$ exposures. We recommend that health impact assessments use the CRFs carefully considering the specific endpoints, location, and policy objectives. For instance, both functional forms could be used to better understand the uncertainties associated with morbidity estimates, such as in regions with low PM$_{2.5}$ concentration. Future work applying these updated CRFs to assess the morbidity burdens and their associated costs can complement previous evaluations of emission policies and provide detailed insights for air quality management.

5. Conclusion

In this paper, we have derived and evaluated updated CRFs for a variety of morbidity endpoints related to short-term PM$_{2.5}$ exposure. We performed a systematic review for seven morbidity endpoints, and used data reported in the reviewed studies to develop CRFs using both log-linear and nonlinear functional forms. We thus relaxed the previous assumption of a linear risk estimate over a narrow exposure range. We quantified uncertainties associated with the CRFs by randomized resampling and Monte-Carlo simulation. We found these CRFs were generally robust to our sensitivity tests. In comparison with previous morbidity CRFs, we showed that our new estimates substantially reduced the range of model uncertainty as well as updating the central estimates. Finally, we showed the global and regional sensitivity to the two different functional forms and discussed the implications for estimation of morbidity impacts. Overall, most of the CRFs discussed here show robustness, especially in comparison with prior studies, though the range of model uncertainty can still be large. They thus can be informative tools for policymaking. However, further efforts should be made to improve these CRFs.

Our study showed that morbidity impact assessment could be very sensitive locally to which functional form was applied, and non-linear CRFs produced significantly higher estimates in most regions of the world for most endpoints. Using the $K_{nl/ll}$ ratios between estimates based on non-linear and log-linear CRFs, we found that regions with low PM$_{2.5}$ showed higher sensitivity to PM$_{2.5}$ for the nonlinear CRFs. Furthermore, in regions with high PM$_{2.5}$ concentrations, the ratio $K_{nl/ll}$ usually ranged between 1 and 3 so that the differences in total number of morbidity cases could be large, indicating the potential for a significant underestimation if only log-linear CRFs are considered. Future analyses of the degree of non-linearity in CRFs will be very valuable.

While future studies of individual morbidity endpoints should be explored to improve our understanding of these concentration–response effects, the CRFs in both functional forms derived in this study can be applied in policy analysis to provide a detailed assessment of the potential economic cost of air pollution.

CRediT authorship contribution statement

Muye Ru: Conceptualization, Methodology, Software, Formal analysis, Visualization, Investigation, Writing – original draft. **Drew Shindell:** Conceptualization, Methodology, Writing – review & editing. **Joseph V. Spadaro:** Writing – review & editing, Resources. **Jean-François Lamarque:** Methodology, Writing – review & editing, Resources. **Ariyani Challapalli:** Investigation, Data curation. **Fabian Wagner:** Conceptualization, Writing – review & editing. **Gregor**

Kiesewetter: Conceptualization, Writing – review & editing.

Declaration of Competing Interest

The authors declare that they have no known competing financial interests or personal relationships that could have appeared to influence the work reported in this paper.

Data availability

Data will be made available on request.

Acknowledgement

Appendix A. Supplementary data

Supplementary data to this article can be found online at https://doi.org/10.1016/j.envint.2023.108122.

References

Bai, L., Shin, S., Burnett, R.T., Kwong, J.C., Hystad, P., Van Donkelaar, A., Goldberg, M. S., Lavigne, E., Copes, R., Martin, R.V., 2019. Exposure to ambient air pollution and the incidence of congestive heart failure and acute myocardial infarction: A population-based study of 5.1 million Canadian adults living in Ontario. Environ. Int. 132, 105004.

Beverland, I.J., Cohen, G.R., Heal, M.R., Carder, M., Yap, C., Robertson, C., Hart, C.L., Agius, R.M., 2012. A comparison of short-term and long-term air pollution exposure associations with mortality in two cohorts in Scotland. Environ. Health Perspect. 120 (9), 1280–1285.

Bowe, B., Xie, Y., Li, T., Yan, Y., Xian, H., Al-Aly, Z., 2018. The 2016 global and national burden of diabetes mellitus attributable to PM2.5 air pollution. Lancet Planet Health 2, e301–e312.

Brook, J.R., Dann, T.F., Burnett, R.T., 1997. The relationship among TSP, PM10, PM2. 5, and inorganic constituents of atmospheric particulate matter at multiple Canadian locations. *JAPCA – J. Air Waste Manag. Assoc.* 47 (1), 2–19.

Burnett, R., Chen, H., Szyszkowicz, M., Fann, N., Hubbell, B., Pope, C.A., Apte, J.S., Brauer, M., Cohen, A., Weichenthal, S., 2018. Global estimates of mortality associated with long-term exposure to outdoor fine particulate matter. Proc. Natl. Acad. Sci. 115, 9592–9597.

Burnett, R.T., Pope, C.A., Ezzati, M., Olives, C., Lim, S.S., Mehta, S., Shin, H.H., Singh, G., Hubbell, B., Brauer, M., Anderson, H.R., Smith, K.R., Balmes, J.R., Bruce, N.G., Kan, H.D., Laden, F., Pruss-Ustun, A., Michelle, C.T., Gapstur, S.M., Diver, W.R., Cohen, A., 2014. An Integrated Risk Function for Estimating the Global Burden of Disease Attributable to Ambient Fine Particulate Matter Exposure. Environ. Health Perspect. 122, 397–403.

Cai, J., Zhao, A., Zhao, J., Chen, R., Wang, W., Ha, S., Xu, X., Kan, H., 2014. Acute effects of air pollution on asthma hospitalization in Shanghai, China. Environ. Pollut. 191, 139–144.

César, A.C.G., Nascimento, L.F., 2018. Coarse particles and hospital admissions due to respiratory diseases in children. An ecological time series study. Sao Paulo Med J 136, 245–250.

Chen, R., Zhou, B., Kan, H., Zhao, B., 2013. Associations of particulate air pollution and daily mortality in 16 Chinese cities: an improved effect estimate after accounting for the indoor exposure to particles of outdoor origin. Environ. Pollut. 182, 278–282.

DeFlorio-Barker, S., Crooks, J., Reyes, J., Rappold, A.G., 2019. Cardiopulmonary effects of fine particulate matter exposure among older adults, during wildfire and non-wildfire periods, in the United States 2008–2010. Environ. Health Perspect. 127 (3), 037006.

Dong, Z., Wang, H., Yin, P., Wang, L., Chen, R., Fan, W., Xu, Y., Zhou, M., 2020. Time-weighted average of fine particulate matter exposure and cause-specific mortality in China: a nationwide analysis. Lancet Planetary Health 4 (8), e343–e351.

Erbas, B., Kelly, A., Physick, B., 2005. Air pollution and childhood asthma emergency hospital admissions: estimating intra-city regional variations. Taylor & Francis 15 (1), 11–20. https://doi.org/10.1080/09603120400018717.

Feng, W., Li, H., Wang, S., Van Halm-Lutterodt, N., An, J., Liu, Y., Liu, M., Wang, X., Guo, X., 2019. Short-term PM10 and emergency department admissions for selective cardiovascular and respiratory diseases in Beijing, China. Sci. Total Environ. 657, 213–221.

Ferreira, T.M., Forti, M.C., De Freitas, C.U., Nascimento, F.P., Junger, W.L., Gouveia, N., 2016. Effects of particulate matter and its chemical constituents on elderly hospital admissions due to circulatory and respiratory diseases. Int. J. Environ. Res. Public Health 13 (10), 947.

Heymann, D., 2009. Bone cancer: progression and therapeutic approaches. Academic Press.

Holland, M., 2014. Cost–benefit Analysis of Final Policy Scenarios for the EU Clean Air Package.

Kelley, M., Schmidt, G.A., Nazarenko, L.S., Bauer, S.E., Ruedy, R., Russell, G.L., Ackerman, A.S., Aleinov, I., Bauer, M., Bleck, R. and Canuto, V., 2020. GISS-E2. 1: Configurations and climatology. *J. Adv. Modeling Earth Syst. 12*(8), e2019MS002025.

Kim, S.Y., Peel, J.L., Hannigan, M.P., Dutton, S.J., Sheppard, L., Clark, M.L., Vedal, S., 2012. The temporal lag structure of short-term associations of fine particulate matter chemical constituents and cardiovascular and respiratory hospitalizations. Environ. Health Perspect. 120 (8), 1094–1099.

Kowalska, M., Skrzypek, M., Kowalski, M., Cyrys, J., Ewa, N., Czech, E., 2019. The relationship between daily concentration of fine particulate matter in ambient air and exacerbation of respiratory diseases in Silesian Agglomeration, Poland. Int. J. Environ. Res. Public Health 16 (7), 1131.

Machin, A.B., Nascimento, L.F., Mantovani, K., Machin, E.B., 2019. Effects of exposure to fine particulate matter in elderly hospitalizations due to respiratory diseases in the South of the Brazilian Amazon. Braz. J. Med. Biol. Res. 52.

McConnell, R., Berhane, K., Gilliland, F., London, S.J., Vora, H., Avol, E., Gauderman, W. J., Margolis, H.G., Lurmann, F., Thomas, D.C., Peters, J.M., 1999. Air pollution and bronchitic symptoms in Southern California children with asthma. Environ. Health Perspect. 107 (9), 757–760.

Murray, C.J., Aravkin, A.Y., Zheng, P., Abbafati, C., Abbas, K.M., Abbasi-Kangevari, M., Abd-Allah, F., Abdelalim, A., Abdollahi, M., Abdollahpour, I., Abegaz, K.H., 2020. Global burden of 87 risk factors in 204 countries and territories, 1990–2019: a systematic analysis for the Global Burden of Disease Study 2019. Lancet 396 (10258), 1223–1249.

Nasari, M.M., Szyszkowicz, M., Chen, H., Crouse, D., Turner, M.C., Jerrett, M., Pope, C. A., Hubbell, B., Fann, N., Cohen, A., 2016. A class of nonlinear concentration-response models suitable for health impact assessment applicable to large cohort studies of ambient air pollution. Air Qual. Atmos. Health 9, 961–972.

Ostro, B.D., 1987. Air pollution and morbidity revisited: a specification test. J. Environ. Econ. Manag. 14, 87–98.

Ostro, B.D., 1989. Estimating the risks of smoking, air pollution, and passive smoke on acute respiratory conditions. Risk Anal. 9, 189–196.

Ostro, B.D., Rothschild, S., 1989. Air pollution and acute respiratory morbidity: an observational study of multiple pollutants. Environ. Res. 50, 238–247.

Pino, P., Walter, T., Oyarzun, M., Villegas, R., Romieu, I., 2004. Fine particulate matter and wheezing illnesses in the first year of life. Epidemiology 702–708.

Silva, A.M.C.D., Mattos, I.E., Ignotti, E., Hacon, S.D.S., 2013. Material particulado originário de queimadas e doenças respiratórias. Revista de Saúde Pública 47, 345–352.

Soleimani, Z., Darvishi Boloorani, A., Khalifeh, R., Griffin, D.W., Mesdaghinia, A., 2019. Short-term effects of ambient air pollution and cardiovascular events in Shiraz, Iran, 2009 to 2015. Environ. Sci. Pollut. Res. 26 (7), 6359–6367.

Spadaro, J. V., Kendrovski, V. & Martinez, G. S. 2018. Achieving health benefits from carbon reductions: Manual for CaRBonH calculation tool.

Strak, M., Weinmayr, G., Rodopoulou, S., Chen, J., De Hoogh, K., Andersen, Z.J., Atkinson, R., Bauwelinck, M., Bekkevold, T., Bellander, T., Boutron-Ruault, M.C., 2021. Long term exposure to low level air pollution and mortality in eight European cohorts within the ELAPSE project: pooled analysis. BMJ 374.

U.S. Environmental Protection Agency. 2015. Environmental Benefits Mapping and Analysis Program–Community Edition (BenMAP-CE): User manual, US Environmental Protection Agency.

U.S. Environmental Protection Agency, 2022. Supplement to the 2019 Integrated Science Assessment for Particulate Matter (Final Report, 2022). Retrieved from https://cfpub.epa.gov/ncea/isa/recordisplay.cfm?deid=354490.

US EPA. PM2.5 Mass Dataset. Federal Land Manager Environmental Database. https://views.cira.colostate.edu/fed/Pub/DatasetDetail.aspx?dssl=1&dsidse=20004.

Van Donkelaar, A., Martin, R. V., Brauer, M., Hsu, N. C., Kahn, R. A., Levy, R. C., Lyapustin, A., Sayer, A. M. & Winker, D. M. 2018. Global Annual PM2.5 Grids from MODIS, MISR and SeaWiFS Aerosol Optical Depth (AOD) with GWR, 1998-2016. Palisades, NY: NASA Socioeconomic Data and Applications Center (SEDAC).

WHO, 2013. Health risks of air pollution in Europe – HRAPIE project. Recommendations for concentration–response functions for cost–benefit analysis of particulate matter, ozone and nitrogen dioxide. https://apps.who.int/iris/handle/10665/153692.

Willers, S.M., Eriksson, C., Gidhagen, L., Nilsson, M.E., Pershagen, G., Bellander, T., 2013. Fine and coarse particulate air pollution in relation to respiratory health in Sweden. Eur Respir J 42, 924–934.

Wong, T.W., Lau, T.S., Yu, T.S., Neller, A., Wong, S.L., Tam, W., Pang, S.W., 1999. Air pollution and hospital admissions for respiratory and cardiovascular diseases in Hong Kong. Occup. Environ. Med. 56 (10), 679–683.

Zhou, X., Cao, Z., Ma, Y., Wang, L., Wu, R., Wang, W., 2016. Concentrations, correlations and chemical species of PM2. 5/PM10 based on published data in China: potential implications for the revised particulate standard. Chemosphere 144, 518–526.